IEEE Access
Multidisciplinary | Rapid Review | Open Access Journal

Received July 5, 2020, accepted July 28, 2020, date of publication July 31, 2020, date of current version August 13, 2020.

Digital Object Identifier 10.1109/ACCESS.2020.3013262

Enhancing Seismic P-Wave Arrival Picking by Target-Oriented Detection of the Local Windows Using Faster-RCNN

ZHENGXIANG HE, PINGAN PENG, LIGUAN WANG, AND YUANJIAN JIANG

School of Resources and Safety Engineering, Central South University, Changsha 410083, China
Digital Mine Research Center, Central South University, Changsha 410083, China

Corresponding author: Pingan Peng (ping_an@outlook.com)

This work was supported by the National Key Research and Development Program of China under Grant 2017YFC0602905.

ABSTRACT The accuracy of P-wave arrival picking is essential for seismic analysis. The improvement in the accuracy of P-wave arrival picking is generally achieved through improved algorithms and the processing of waveforms. Therefore, we propose a method that uses deep learning to detect local windows to enhance the accuracy of P-wave arrival picking. The local window is defined as a short time window containing the main components of the signal. The faster-RCNN model is trained on the dataset with the calibrated local window. The trained faster-RCNN model is used for the local window detection of new records, and the existing algorithm is going to work in the local window. As a validation, four kinds of automatic P-wave arrival picking algorithms (wavelet-transform-based approach, PphasePicker algorithm, STAFD/LTAFD algorithm, and deep learning method) are used to conduct experiments in synthetic seismic records and field seismic records, respectively. The field experimental results show that the method proposed in this article can improve the picking capacity of the four methods by 17.5%, 37.6%, 62.4%, and 46.8%, respectively. No matter which algorithm is used, the accuracy of P-wave arrival picking in the local window is generally enhanced. The method presented in this article has a positive effect on improving the accuracy of seismic records.

INDEX TERMS P-wave arrival picking, deep learning, faster-RCNN, local window, seismic records.

I. INTRODUCTION

P-wave arrival picking is a crucial step in seismic analysis, and it is the premise of the event location, source mechanisms calculation, origin time determination, and subsurface velocity inversion. Nevertheless, the P-wave picking has always been a drag in the whole seismic analysis process. With the continuous economic investment, the sources of seismic data acquisition are becoming broader, and the amount of data is gradually increasing. Manual P-wave arrival picking has become a very exhausting task for analysts. Therefore, finding a way to pick the P-wave arrival automatically and accurately is not only suitable for earthquake early warning but also allows analysts to shift their energy to more meaningful tasks.

For a long time, many methods have been proposed to automate the P-wave picking and have achieved excellent results. These methods can be roughly divided into traditional numerical calculation methods and emerging artificial intelligence methods. The most typical of numerical calculation methods are STA/LTA (short and long time ratio) [1] and AIC (Akaike information criterion) [2]. STA/LTA uses the sliding time window to calculate the characteristic curve, while AIC calculates it using the entire given time series. Based on these two classic algorithms, many improved algorithms have been derived, such as MER (Modified energy ratio) [3], [4], MCM (Modified Coppens' method) [5], [6], PAL-K (Phase arrival identification - Kurtosis) [7], [8], S/L-Kurt (Short-term kurtosis to long-term kurtosis ratio) [9], JER (Joint energy ratio) [10], [11], wavelet-transform-based approaches [12], [13], and waveform cross-correlation methods [14]–[16]. Over the past decades, these traditional numerical calculation methods have played an essential role in seismic monitoring.

Although the traditional numerical calculation methods performed very well, they are still not fully automated in practical applications because of the influence of signal quality. Thanks to the rapid development of computers, a new class of P-wave arrival picking methods with high robustness

The associate editor coordinating the review of this manuscript and approving it for publication was Sudhakar Babu Thanikanti.

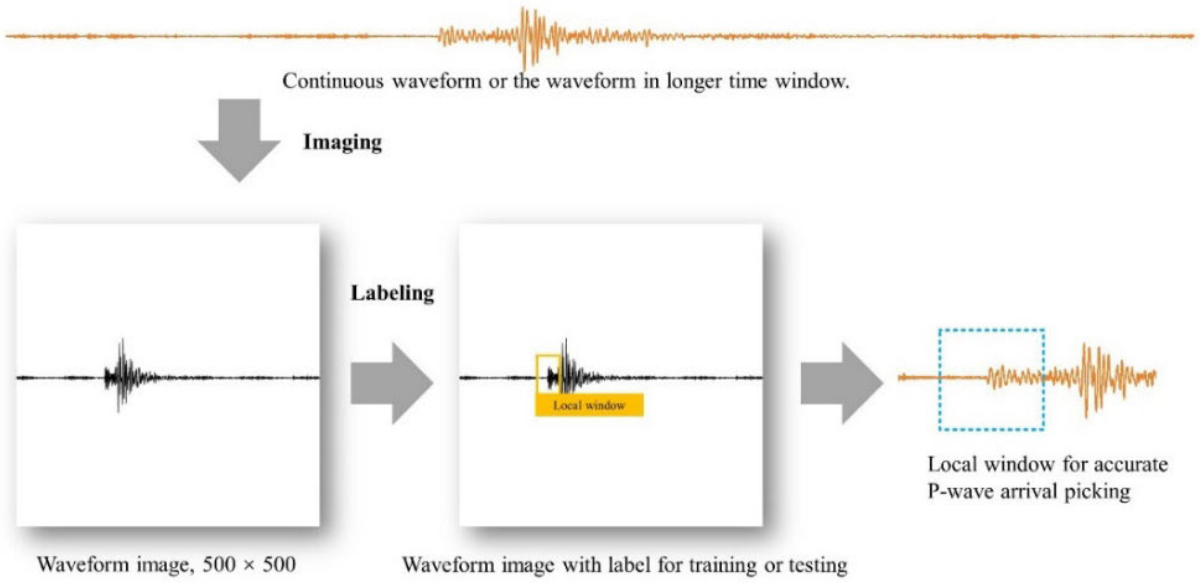

FIGURE 1. Data preprocessing.

based on artificial intelligence technology has been continuously proposed. Since the 1990s, machine learning and neural network have been applied to pick seismic arrival, leverage a data-driven approach to provide many new ideas for seismic analysis [17]–[19]. Chen [20] tried to use unsupervised machine learning to promote the quality of P-wave arrival picking by dividing data into noise and signal segments. With the rise of deep learning, Perol *et al.* [21] proposed a CNN (convolutional neural network) model for earthquake detection and location; Ross *et al.* [22] trained two CNN models to pick the first seismic arrival and get the first motion, respectively; and Zhu *et al.* [23] and Chen *et al.* [24] creatively treat the phase picking as a classification problem and enhance the P-wave picking after a rough classification using a CNN. In addition to CNN, RNN (recurrent neural network) is also used in P-wave arrival picking attempts, such as Mousavi *et al.* [25] combined a CNN and an RNN to detect earthquake signals and achieved high-detection accuracy with a low rate of false positives, and Zhou *et al.* [26] developed a hybrid algorithm using both convolutional and recurrent neural networks to pick phases from archived continuous waveforms. Moreover, in the latest research, Qu *et al.* [27] compared the usability of machine learning and deep learning in the seismic P-wave arrival picking and analyzed the applicability of the two approaches.

Most of the abovementioned picking algorithms were applied in seismic monitoring based on a local-window strategy [28]. The local window strategy is to pick the P-wave arrival within a limited time window, and the length of the local window affects the accuracy and availability of the adopted approach. For example, Zhang *et al.* [29] developed an automatic P-wave arrival picking algorithm based on the wavelet transform and AIC picker, and the modified AIC picker is applied at the given local window. This example is not unique. Ross *et al.* [22] applied a CNN to P-wave arrival picking problems using a large amount of training data, and these training data are waveform segments. Each waveform segment is a local window containing only 400 samples points. Therefore, we propose a targeted detection approach of the local window based on faster R-CNN (regions with convolutional neural networks) to enhance the performance of existing picking algorithms by quickly detecting the local window of P-wave arrival in continuous waveforms or longer time windows.

II. MATERIALS AND METHODS

A. DATA

We chose the records of 7,014 earthquakes recorded by the NCEDC (Northern California Earthquake Data Center, 2014) from January 1, 2016 to June 1, 2016 at 34 EGS stations [30]. The data are a mixture of DPE, DPN, and DPZ channels. These seismic records are associated with manually determined P-wave picks. These records are converted into pictures during the application of the method proposed in this article, and the results obtained in the form of pictures are converted back into waveforms for arrival picking. This data processing as shown in Fig. 1. The original waveform data will be plotted and saved as a picture of uniform size. For experimental purposes, these pictures will be processed using some marking software so that they carry a ground truth of the local window.

B. FASTER R-CNN

Faster R-CNN (regions with convolutional neural networks) was proposed via Ross Girshick in 2015 [31], [32]. Based on traditional object detection methods, faster R-CNN integrates

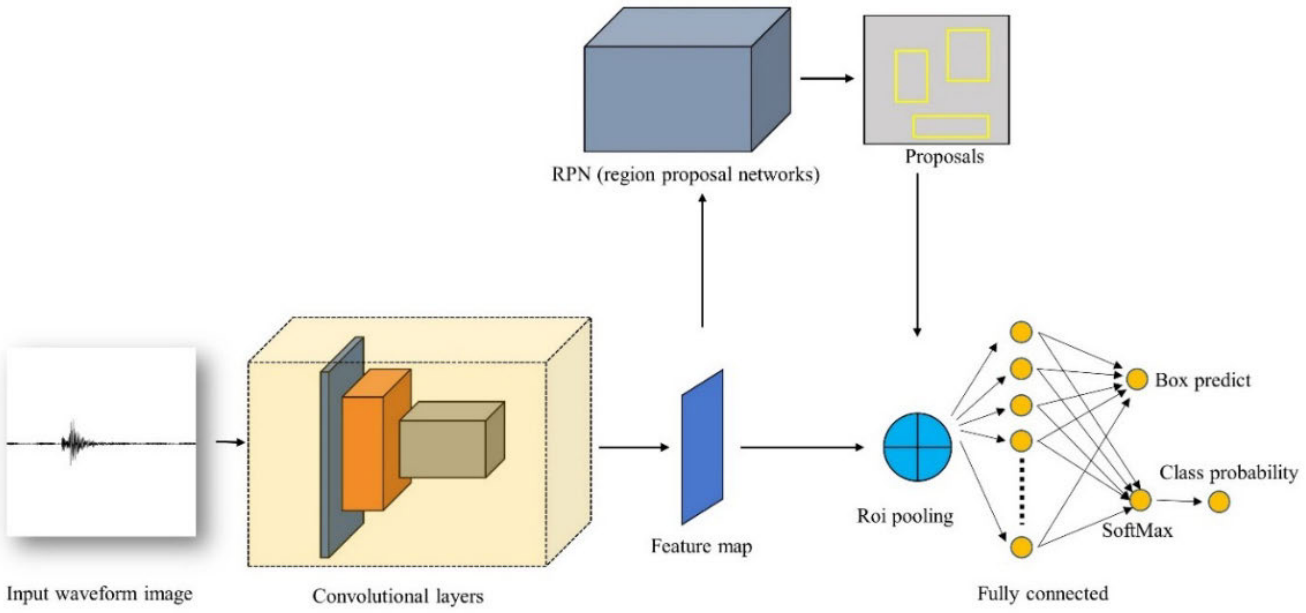

FIGURE 2. The architecture of faster-RCNN.

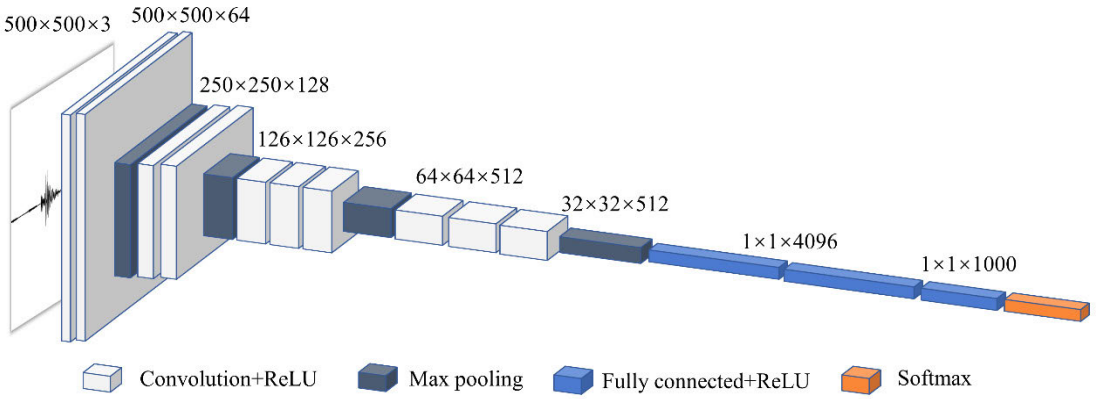

FIGURE 3. The architecture of VGG16 (Visual Geometry Group Network 16).

feature extraction, proposal extraction, bounding box regression (rectangle refine), and classification into one network, which makes the overall performance greatly improved, especially in the detection speed. Faster R-CNN is composed of two modules. The first module is a deep fully convolutional network that proposes regions, and the second module is the Fast R-CNN detector that uses the proposed regions. More detail, faster R-CNN can be considered to be composed of four parts, namely convolutional layers, RPN (region proposal networks) [33], Roi pooling, and classification. Fig. 2 shows the architecture diagram of faster R-CNN.

Unlike machine learning, deep learning does not need to give features before training but automatically extracts features from the input data by the convolutional operation. Therefore, in faster R-CNN, the first step is feature maps extraction from input via the convolutional layers. The feature map extraction network used in this article is VGG16 (Visual Geometry Group Network 16), a deep learning network consisting of 13 convolutional layers and 3 fully-connected layers (as shown in Fig. 3). However, we will not use the entire VGG16 architecture, and we choose the last ReLU (Rectified Linear Unit) output before entering the fully connected layer as the feature map. In fact, any kind of convolutional neural network and any node in its structure can be used as a feature map. The feature maps are shared for subsequent RPN layers and fully connected layers. The RPN is used to generate region proposals. This network uses the softmax layer to determine whether anchors are positive or negative and then uses bounding box regression to modify anchors to obtain accurate proposals. Fig. 4 shows the specific structure of the RPN. It can be seen that the RPN is divided into two independent steps. Among them, one step classifies anchors

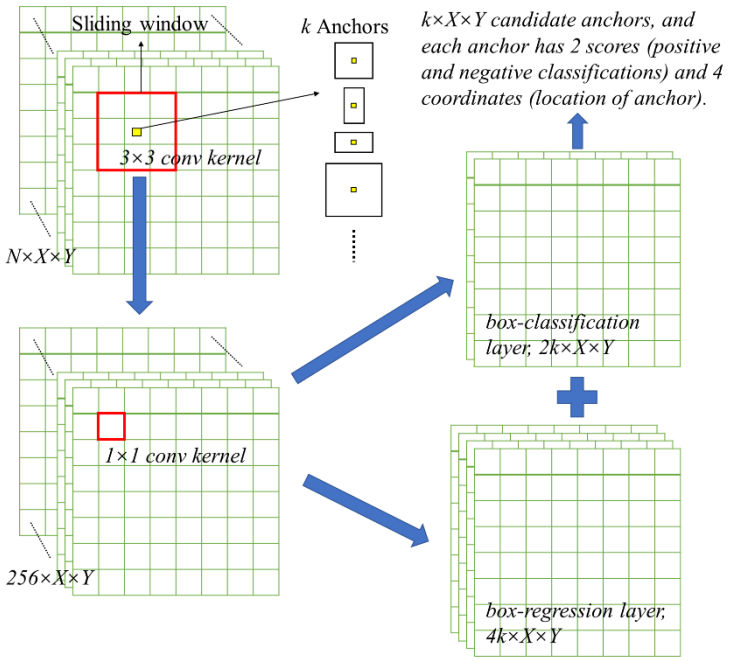

FIGURE 4. Data flow and architecture of RPN (Region Proposal Networks).

into positive and negative classifications, and the other one calculates the bounding box regression offset to obtain an accurate proposal. After this processing, the feature maps converted into scoring anchors (proposals) of different sizes. The obtained feature maps and proposals are sent to the Roi pooling layer, and the proposal feature maps are extracted through the comprehensive information of the Roi pooling layer. As the input of the fully connected layer, the proposal feature maps are classified and evaluated to determine the location of the local window.

C. P-WAVE ARRIVAL PICKING ALGORITHM

To evaluate the effect of targeted detection the local window via faster-RCNN on the accuracy of P-wave arrival picking, we have selected some reliable and the state of the art algorithms for testing. These algorithms include STAFD/LTAFD (short-term kurtosis to long-term kurtosis ratio) proposed by Li *et al.*, wavelet-transform-based approach proposed by Zhang *et al.*, PphasePicker algorithm proposed by Erol Kalkan, and deep learning method proposed by Ross *et al.* In this section, we give a brief introduction to these methods.

1) STAFD/LTAFD

STA/LTA method is a very typical P-wave arrival picking method, and many existing methods are modified based on it. Saragiotis *et al.* [34] found that if a signal contains a non-Gaussian wave, it can be effectively identified by using kurtosis. However, the kurtosis picker is overly reliant on the length of the waveform window. Therefore, Zhang *et al.* [35] proposed an STAFD/LTAFD fractal dimension algorithm that integrates the advantages of STA/LTA and kurtosis picker. The STAFD and LTAFD windows preceding the mth time index are computed as follows:

$$\mathrm{STAFD}(m)/\mathrm{LTAFD}(m) = \frac{\sum_{i=m-ns+1}^{m} \mathrm{CF}(i)/ns}{\sum_{i=m-nl+1}^{m} \mathrm{CF}(i)/nl} \tag{1}$$

where CF is the characteristic function, and it is given as

$$\mathrm{CF}(k) = d(k)^2 + [d(k) - d(k-1)]^2 \tag{2}$$

here, $d(k)$ is the fractal dimension at point k, and k is the ordinal of the data point that starts from the second point as an integer.

2) WAVELET-TRANSFORM-BASED APPROACH

Like STA/LTA, AIC picker is a typical algorithm, but it is also not perfect [36]. The AIC picker is very limited by the SNR (signal-to-noise ratio). When the SNR is relatively small, the effect of arrival picking is weak. Therefore, Zhang *et al.* [29] proposed a modified AIC picker combined with wavelet transform. A single seismic record is transformed into multi-scale wavelet coefficients by the wavelet transform. Thus, AIC picker can work on wavelet coefficients of different scales. The process and results of the P-wave arrival picking based on the wavelet-transform-based approach are shown in Fig. 5.

3) PPHASEPICKER ALGORITHM

Kalkan [37] proposed a new approach for picking P-wave arrival time without requiring detection interval or threshold settings. The PphasePicker algorithm transforms the

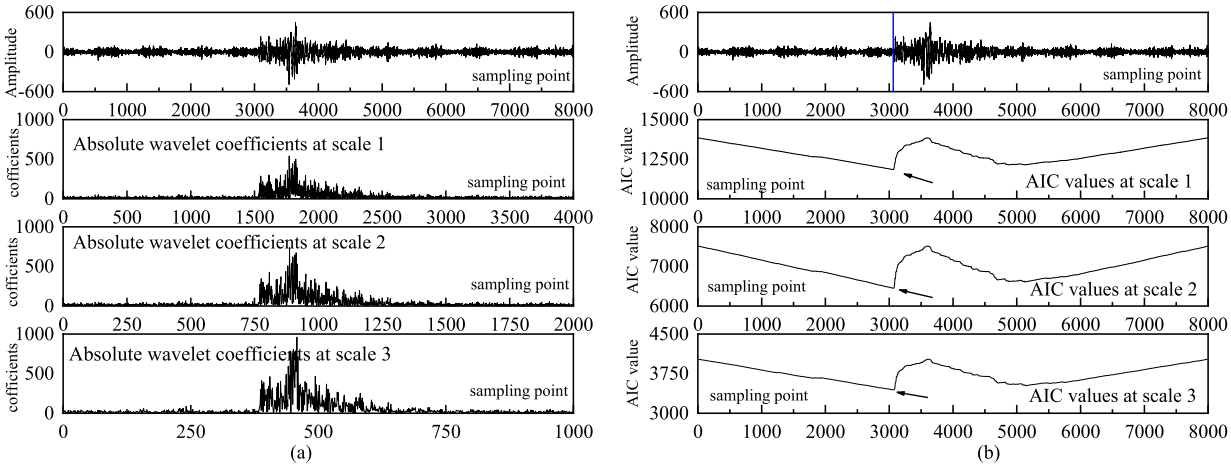

FIGURE 5. Wavelet-transform-based AIC picker.

record into a response domain of a single-degree-of-freedom (SDOF) oscillator with viscous damping and then tracks the rate of change of dissipated damping energy to pick P-wave arrival. The algorithm is described step-by-step in the following:

a. Determine the maximum and minimum amplitudes, $y_{\max}$ and $y_{\min}$, of the power of damping energy, which will correspond to lower and upper state levels.

b. Calculate the amplitude range y_R of the power of damping energy using $y_R = y_{\max} - y_{\min}$.

c. For the specified number of histogram bins (M), determine the bin width Δy as the ratio of the amplitude range to the number of bins; Δy is found by dividing y_R by M.

d. Sort the data values into the histogram bins.

e. Identify the lowest-indexed histogram bin (i_{low}) and the highest-indexed histogram bin (i_{high}) with nonzero counts.

f. Divide the histogram into two sub-histograms. The indexes of the lower histogram bins are $i_{\text{low}} \leqslant i \leqslant 1/2 \times (i_{\text{high}} - i_{\text{low}})$, and the indexes of the upper histogram bins are $i_{\text{low}} + 1/2 \times (i_{\text{high}} - i_{\text{low}}) \leqslant i \leqslant i_{\text{high}}$.

g. The low-state level, which is the mode of the largest bin within the lower histogram, corresponds to the P-wave arrival, and its onset is determined as the last zero-crossing on the filtered seismogram before the P-wave arrival.

4) DEEP LEARNING METHOD

The components of seismic signals are complex, and it is often difficult to adapt to the needs of arrival picking of various signals using mathematical calculation methods, which is why most existing algorithms are currently semi-automated. However, with the development of artificial intelligence technology, deep learning methods have provided a new idea for the arrival picking of seismic records. Ross *et al.* [22] proposed an intelligent P-wave arrival picking method based on the convolutional neural network. This Picker is a convolutional neural network (as shown in Fig. 6) built for P-wave arrival picking and uses waveforms directly as input. Therefore, a local window must be determined before using this method; otherwise, it will take longer calculation time and poor picking results.

III. EXPERIMENTS AND RESULTS

To verify the effectiveness of the proposed method, we designed two experiments. One is based on synthetic data, and another is based on field data. In these two experiments, it was demonstrated that the local window detection via faster-RCNN could enhance the ability of the P-wave arrival picking.

A. SYNTHETIC EXPERIMENTS

The beauty of synthetic experiments is that we have the ground-truth solution, and thus, the comparison is more intuitive. We simulated a series of seismic records using the Ricker wavelet and forward modeling of P-wave arrival. There is a difference between them by adding gaussian random noise. A synthetic seismic record shown in Fig. 7. The synthetic seismic dataset is simulated from a six layers velocity model with the random sources and 50 receivers, as shown in Fig. 8. The 50 traces correspond to the recorded data of 50 evenly spaced recorders, shown in Fig. 9.

We moved the source's distance between 1 m and 3000 m, take a value every 15 m. Move the source's depth between 1000 m and 1500 m, and also take a value every 15 m. Thus, there will be a total of 10400 sources and 520000 traces. Some of these synthetic records are used to train faster R-CNN, and others are used to verify the effectiveness of the method proposed in this article. Two steps are taken for the proposed method to enhance P-wave arrival picking. We trained the faster R-CNN to find the local window. The local window is a very short time window containing the P-wave arrival, and the example is shown as Fig.10(a) (and Fig.10(b) is the ground truth of synthetic seismic records). After training faster R-CNN, we use the trained model to find the local window

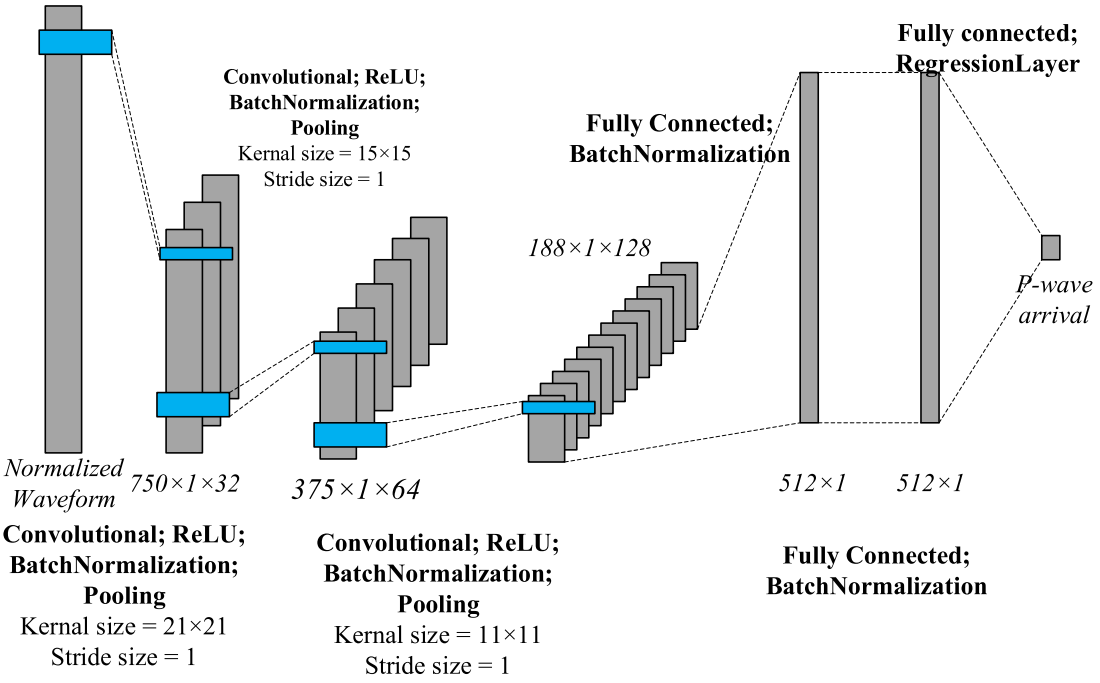

FIGURE 6. The data flow and architecture of a CNN picker.

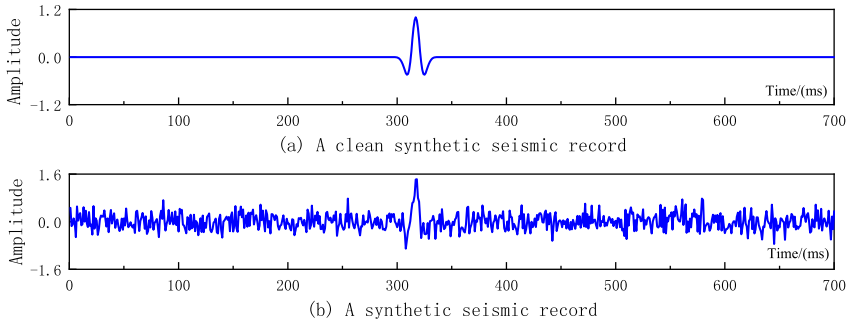

FIGURE 7. The example of a synthetic seismic record. Each synthetic seismic record is generated based on the first arrival time and different SNR based on the Ricker wavelet.

of the synthetic records and perform P-wave arrival picking in the local window.

We compare the picking results with 20,000 synthetic records, and a detailed example is a record inspired by the source in (2500, 1400). Four P-wave arrival picking algorithms presented in section 2.3 are worked on the entire record and local window at the same time. Moreover, to numerically evaluate the performance, we use the arrival picking error metric, which is defined as follows:

$$Error = T_p - T_t \tag{3}$$

where T_p is the arrival picking by algorithm, T_t is the ground truth. Moreover, we defined a metric to describe the enhancement of P-wave arrival picking by using the method proposed in this article. The enhancement metric is defined as:

$$EM = \frac{N_{|Error|<=\varepsilon} - M_{|Error|<=\varepsilon}}{N_{|Error|<=\varepsilon}} \tag{4}$$

where ε is the target accuracy, here $\varepsilon = 0.05s$; $M_{|Error|<=\varepsilon}$ is the count of the absolute error metric less than ε, and the error metric is calculated on the complete waveforms; $N_{|Error|<=\varepsilon}$ is the count of the absolute error metric less than ε, and the error metric is calculated on the local windows detected by faster-RCNN. Fig. 11 and Table 1 show the picking results between non-local-window picking and local-window picking, and all of them based on 20,000 synthetic records. For the wavelet-transform-based approach, $M_{|Error|<=0.05} = 32$, $N_{|Error|<=0.05} = 20000$, and EM = 99.8%. For the PphasePicker algorithm, $M_{|Error|<=0.05} = 1039$, $N_{|Error|<=0.05} = 20000$, and EM = 94.8%. For the STAFD/LTAFD algorithm, $M_{|Error|<=0.05} = 319$, $N_{|Error|<=0.05} = 20000$, and EM = 98.4%. And for the deep learning method, $M_{|Error|<=0.05} = 2655$, $N_{|Error|<=0.05} = 20000$, and EM = 86.7%. It can be seen from Fig. 11 that no matter which picking algorithm is used, the error metric of the picking results based on the local window is reduced

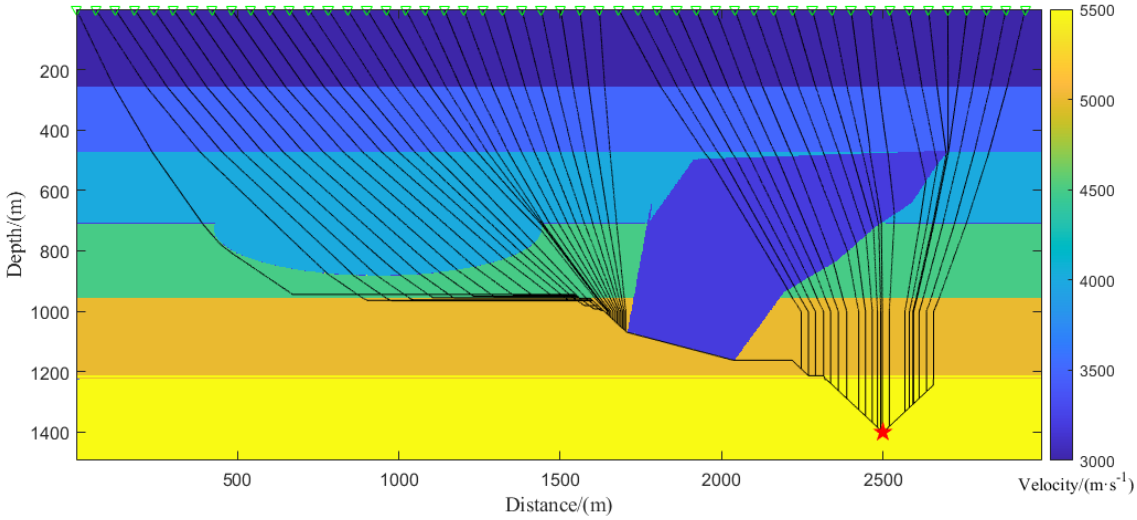

FIGURE 8. The geometry of the synthetic example.

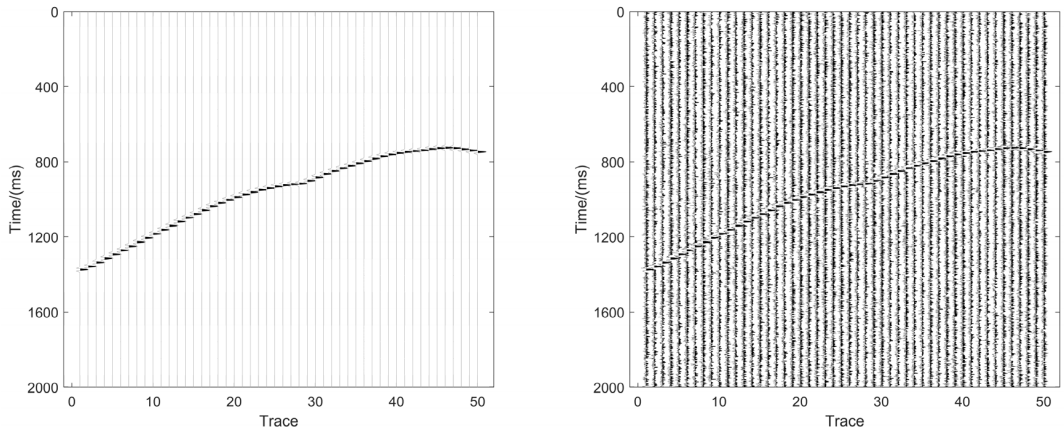

FIGURE 9. The waveforms of a synthetic seismic event.

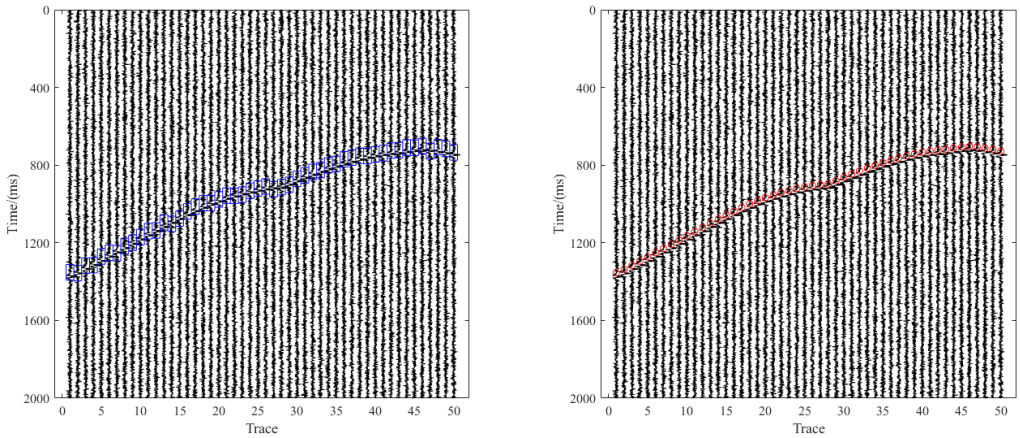

FIGURE 10. The results of finding local windows by faster-RCNN and the ground truth of synthetic records. The blue rectangles in (a) are the local windows recognized by faster-RCNN. The red circles in (b) are the ground truth of synthetic P-wave arrival.

by an order of magnitude. Moreover, the EM of each picking method is greater than 0. This means that the method proposed in this article has the enhancement effect for P-wave arrival picking.

In order to more intuitively show the enhanced effect of using faster-RCNN to detect the local window for seismic P-wave arrival picking, we performed P-wave arrival picking on a synthetic record shown in Fig. 10 and compared the

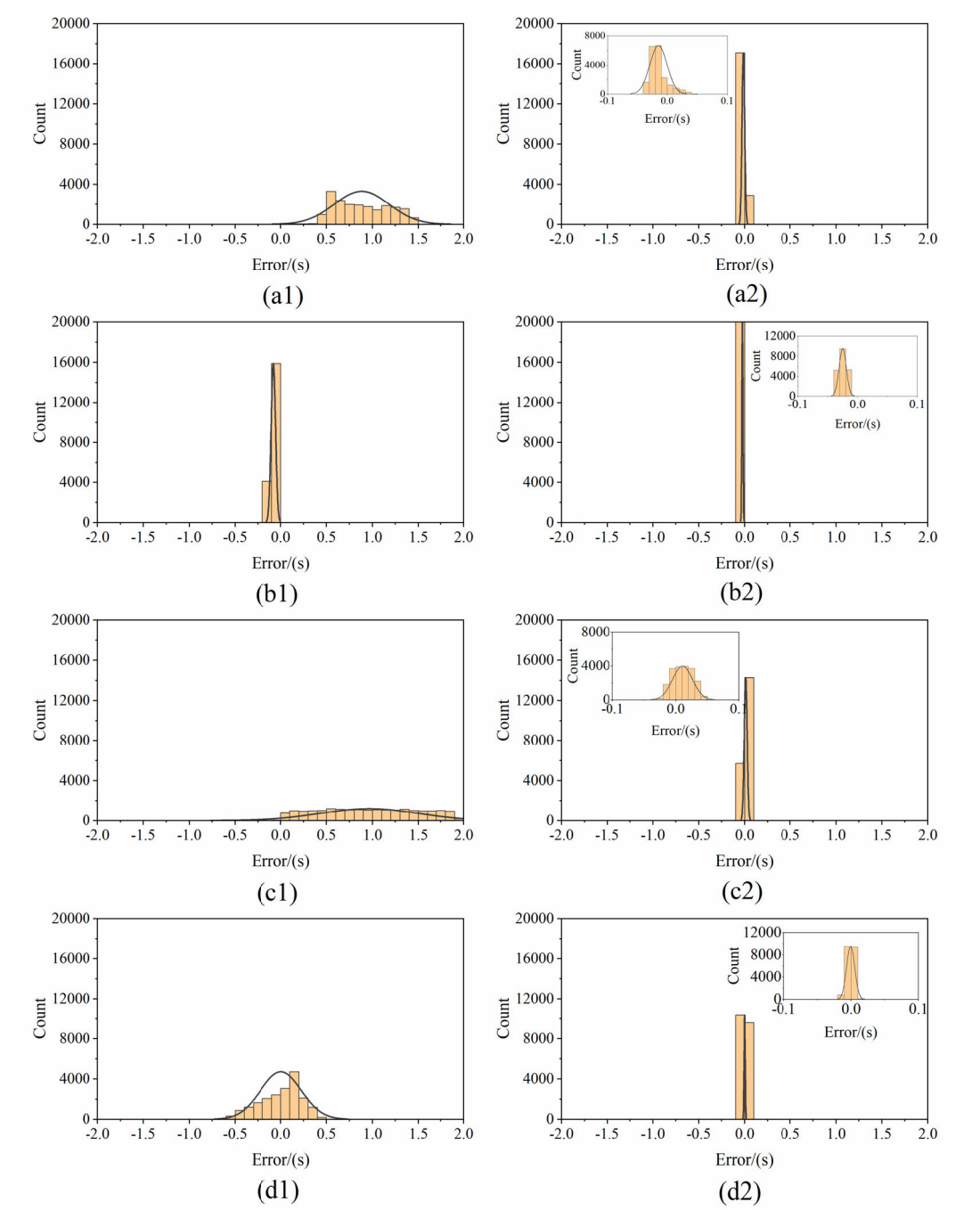

FIGURE 11. The picking results between non-local-window picking and local-window picking. (a1) the non-local-window picking results of the wavelet-transform-based approach. (a2) the local-window picking results of the wavelet-transform-based approach and the local window is detected by faster-RCNN. (b1) the non-local-window picking results of the PphasePicker algorithm. (b2) the local-window picking results of the PphasePicker algorithm and the local window is detected by faster-RCNN. (c1) the non-local-window picking results of the STAFD/LTAFD algorithm. (c2) the local-window picking results of the STAFD/LTAFD algorithm and the local window is detected by faster-RCNN. (d1) the non-local-window picking results of CNN picker. (d2) the local-window picking results of CNN picker and the local window is detected by faster-RCNN.

results. As shown in Fig.12, there are four groups of comparative experimental results. Firstly, P-wave arrival picked on the complete waveform using various picking methods, the red triangles in Fig.12(a), Fig.12(b), Fig.12(c), and Fig.12(d) are the P-wave arrival picking results of different traces. In Fig.12(a), the maximum error is 0.4693 s, the smallest error is 0.0004 s, the mean error is 0.0534 s, and there are 17 traces with an error of less than 0.03s. In Fig.12(b), the maximum

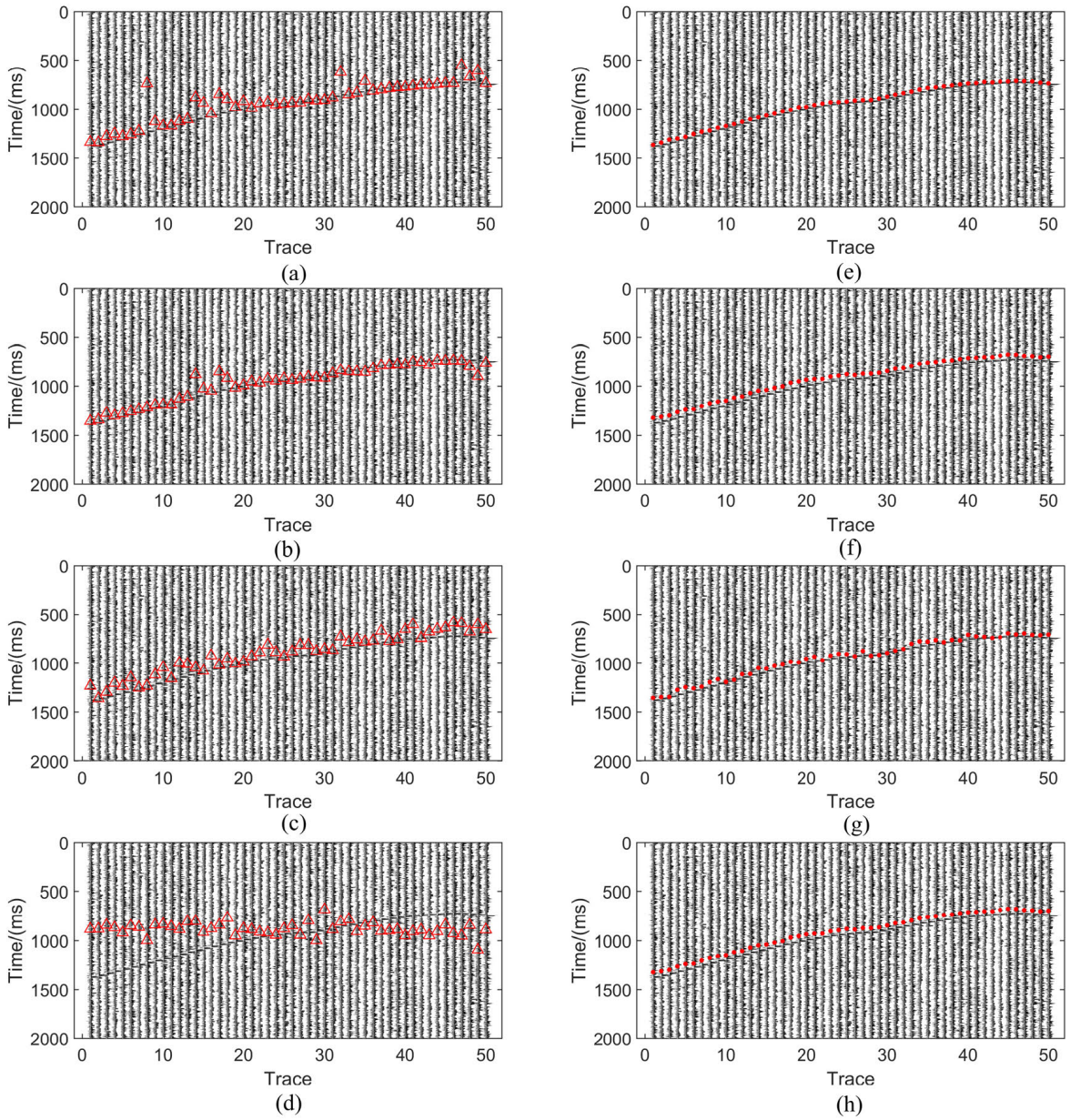

FIGURE 12. The comparative experimental results of P-wave arrival picking of one seismic event. The red triangles are P-wave arrival picking results on the complete waveform by different picking methods: (a) wavelet-transform-based approach, (b) PphasePicker algorithm, (c) STAFD/LTAFD algorithm, and (d) Deep learning method. The red points are P-wave arrival picking results on the local window by different picking methods: (e) wavelet-transform-based approach, (f) PphasePicker algorithm, (g) STAFD/LTAFD algorithm, and (h) Deep learning method.

error is 0.1983 s, the smallest error is 0.0007 s, the mean error is 0.0367 s, and there are 25 traces with an error of less than 0.03s. In Fig.12(c), the maximum error is 0.1256 s, the smallest error is 0.0012 s, the mean error is 0.0559 s, and there are only 20 traces with an error of less than 0.03s. In Fig.12(d), the maximum error is 0.4748 s, the smallest error is 0.0099 s, the mean error is 0.1885 s, and there are 4 traces with an error of less than 0.03s. In this experiment, it can be found that when various methods are used to pick the P-wave arrival on a long time series, a significant error often occurs, which is very unfavorable for analysis of the focal mechanism. Secondly, we use the trained faster-RCNN to detect the local window containing the subject of the signal in the waveform and picking the P-wave arrival in the local window. The red points in Fig.12(e), Fig.12(f), Fig.12(g), and Fig.12(h) are the P-wave arrival picking results in the local window of different traces. In Fig.12(e), the maximum error is 0.0103 s, the smallest error is 0.0003 s, the mean error is 0.0056 s, and there are 50 traces with an error of less than 0.03 s. In Fig.12(f), the maximum error is 0.0345 s, the

TABLE 1. The synthetic picking results between non-local-window picking and local-window picking.

Method	complete waveform $M_{\|Error\|<=0.05}$	local window $N_{\|Error\|<=0.05}$	$EM = \frac{N_{\|Error\|<=\varepsilon} - M_{\|Error\|<=\varepsilon}}{N_{\|Error\|<=\varepsilon}}$
Wavelet-transform-based approach	32	20000	99.8%
PphasePicker algorithm	1039	20000	94.8%
STAFD/LTAFD algorithm	319	20000	98.4%
Deep learning method	2655	20000	86.7%

smallest error is 0.0147 s, the mean error is 0.0249 s, and there are 36 traces with an error of less than 0.03 s. In Fig.12(g), the maximum error is 0.0343 s, the smallest error is 0.0003 s, the mean error is 0.0163 s, and there are 46 traces with an error of less than 0.03 s. In Fig.12(h), the maximum error is 0.0327 s, the smallest error is 0.0128 s, the mean error is 0.0231 s, and there are 42 traces with an error of less than 0.03s. The experimental results show that even though there are still differences in the accuracy of the P-wave picking results, the picking accuracy of all methods is greatly enhanced. Finally, through the analysis and comparison of each method, it can be found that the P-wave picking method based on deep learning has a better effect. If we need to get better picking results, we must increase the amount of data for training. In general, through synthesis experiments, it can be found that it is feasible to use faster-RCNN to detect local windows to enhance the P-wave picking accuracy.

B. FIELD SEISMIC DATA

We also test the approach proposed in this article with a real field seismic dataset. The field seismic dataset we used was recorded by the NCEDC.

Similar to the synthetic example, three steps are taken to carry out the proposed enhanced picking method in field seismic data. Firstly, we divide the data into a training set (5,894 waveforms) and test set (1,030 waveforms), and the P-wave arrival is picked on the complete waveform in test sets. Based on the prepared data set, we started to train faster-RCNN. We set the training process that will end in 40 Epochs; the size of the mini-batch is 5. Furthermore, the Sgdm (Stochastic gradient descent momentum) optimizer is used for the training process, and the initial learning rate is 0.001; and the entire training process requires 168 minutes and 18 seconds on one NVIDIA RTX 2080 GPU. Secondly, we train the faster-RCNN with the training set and the calibrated local window, and detect the local window of the records in the test set. Finally, the P-wave arrival is picked on the local window of each record in test sets, and compared with the results of the first step. Fig. 13 shows the picking results between non-local-window picking and local-window picking, and both based on 1030 field seismic records. Similarly, we use *EM* (equation 5) to evaluate the enhancement of the method proposed in this article, and due to the sampling rate is 500 Hz, therefore, we choose $\varepsilon = 0.1$ s as the target accuracy. As shown in Fig.13 and Table 2, for wavelet-transform-based approach, $M_{|Error|<=0.1} = 713$, $N_{|Error|<=0.1} = 864$, and EM = 17.5%. For PphasePicker algorithm, $M_{|Error|<=0.1} = 506$, $N_{|Error|<=0.1} = 811$, and EM = 37.6%. For STAFD/LTAFD algorithm, $M_{|Error|<=0.1} = 80$, $N_{|Error|<=0.1} = 213$, and EM = 62.4%. And for deep learning method, $M_{|Error|<=0.1} = 25$, $N_{|Error|<=0.1} = 47$, and EM = 46.8%. It can be seen from Fig. 13 that no matter which picking algorithm is used, the error of the picking results based on the local window is all converge to 0 s.

Moreover, Fig.14 shows a field seismic event that occurred at 23: 3: 35 on March 31, 2016. This event contained a total of 102 waveforms, but because some waveforms were not seismic waveforms (or the signal-to-noise ratio was too low), we deleted them, and eventually 84 waveforms participated in the experiment. As shown in Fig.14, there are four groups of comparative experimental results. The red circles are P-wave arrival picking results on the complete waveform by different picking methods: (a) wavelet-transform-based approach, (b) PphasePicker algorithm, (c) STAFD/LTAFD algorithm, and (d) Deep learning method. The red rectangles are P-wave arrival picking results on the local window by different picking methods: (a) wavelet-transform-based approach, (b) PphasePicker algorithm, (c) STAFD/LTAFD algorithm, and (d) Deep learning method. Moreover, the detailed results of comparative experiments are shown in table 1. It can be seen that the picking results using the enhanced P-wave picking method proposed in this article is better than the original picking method.

IV. DISCUSSION

Based on the above experimental results, it can be found that picking P-wave arrival in a short time window (local window) greatly enhanced the accuracy of the picking algorithm. Therefore, based on this conclusion, we explored the relationship between the length of the time window and the picking accuracy. Each waveform in the test set was intercepted to change the time window length of the waveform. The number of sampling points of the new waveform was 1000, 2000, 3000, 4000, 5000, 6000, and 7000, respectively. Although the waveform length was reduced, the main components of the seismic signal were still included. The P-wave arrival of each waveform in different lengths of the time window is picked,

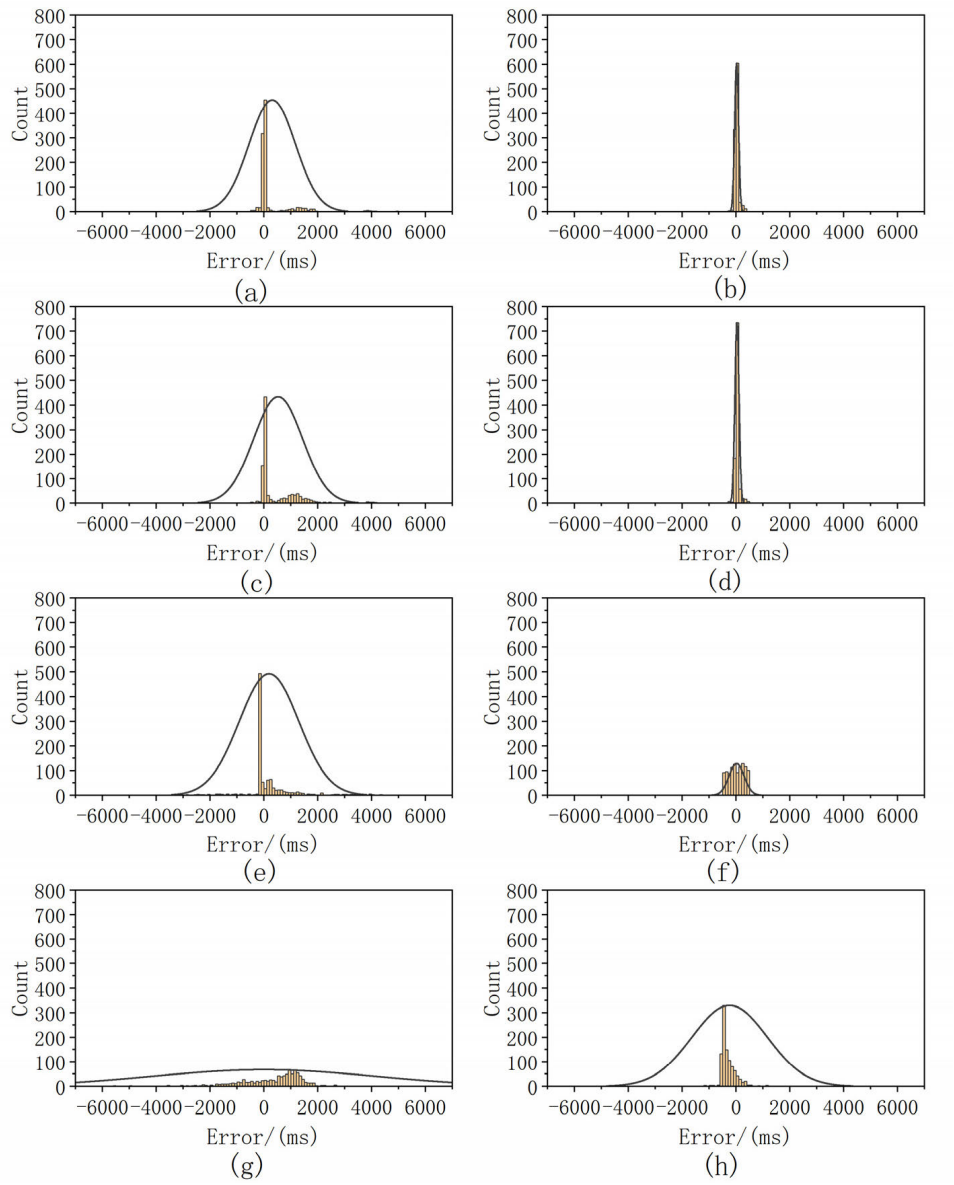

FIGURE 13. The field seismic data picking results between non-local-window picking and local-window picking. (a) the non-local-window picking results of the wavelet-transform-based approach. (b) the local-window picking results of the wavelet-transform-based approach and the local window is detected by faster-RCNN. (c) the non-local-window picking results of the PphasePicker algorithm. (d) the local-window picking results of the PphasePicker algorithm and the local window is detected by faster-RCNN. (e) the non-local-window picking results of the STAFD/LTAFD algorithm. (f) the local-window picking results of the STAFD/LTAFD algorithm and the local window is detected by faster-RCNN. (g) the non-local-window picking results of CNN picker. (h) the local-window picking results of CNN picker and the local window is detected by faster-RCNN.

and SE (Sum of Error) is introduced for evaluation [20]. The calculation method of SE is:

$$\mathrm{SE} = \sum_{h=1}^{H} |I_p(h) - I_t(h)| \tag{5}$$

where, $I_p(h)$ denotes the picked arrival time of the h-th record in the dataset, $I_t(h)$ denotes the corresponding actual arrival time of the h-th record in the dataset, H denotes the number of records in the dataset, here $H = 1030$.

As shown in Fig.15, a clear rule is that when the waveform size decreases, even without any preprocessing (such as filtering), the accuracy of P-wave arrival piking is gradually improved. The principle of this phenomenon is also easy to explain. When the waveform length is short, the interference information is significantly reduced, the proportion of main components increased, and the effect of the P-wave arrival picking is enhanced. However, in the actual operation process, it is difficult to determine such

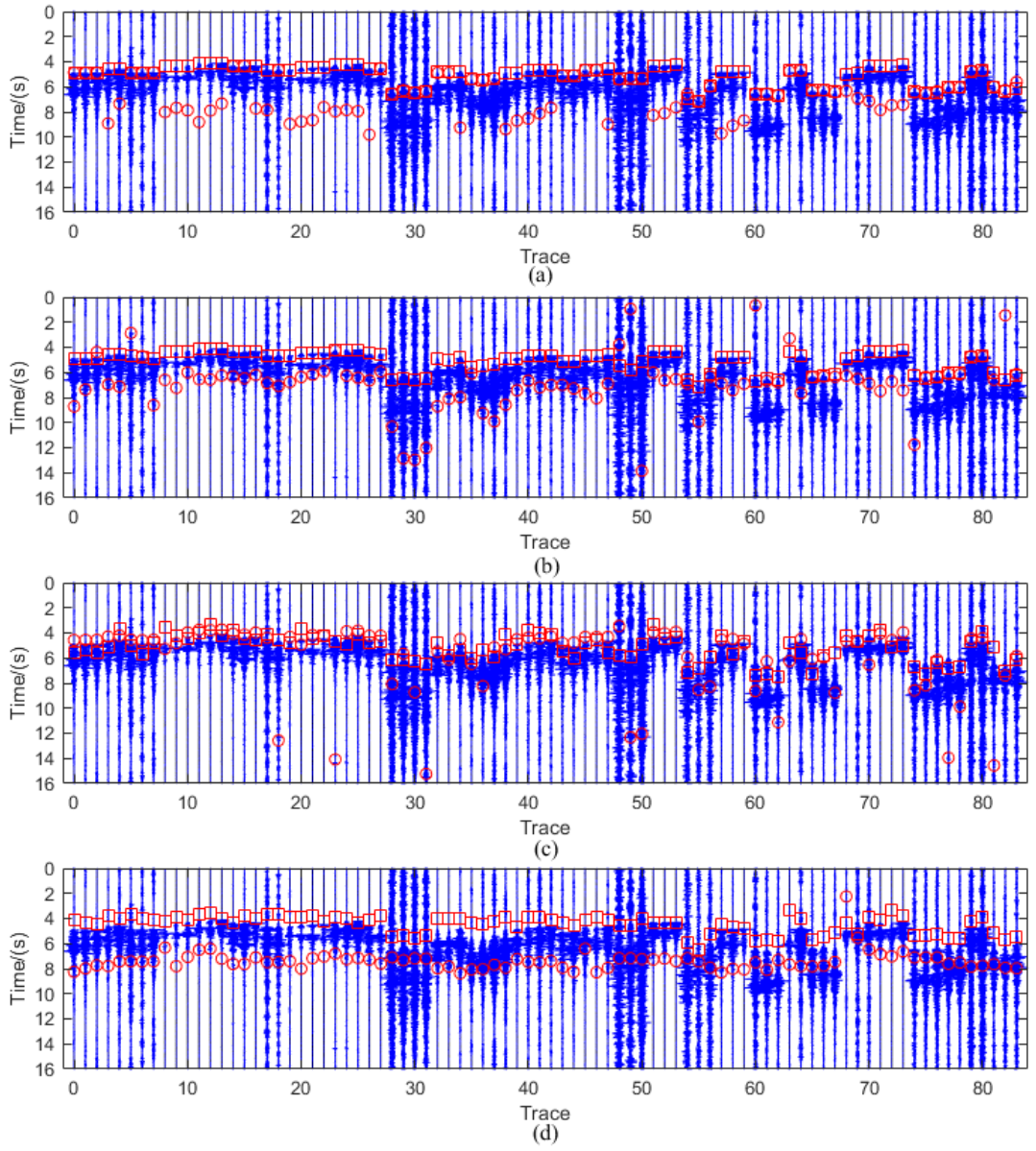

FIGURE 14. The comparative experimental results of P-wave arrival picking of one field seismic event. The red circles are P-wave arrival picking results on the complete waveform by different picking methods: (a) wavelet-transform-based approach, (b) PphasePicker algorithm, (c) STAFD/LTAFD algorithm, and (d) Deep learning method. The red rectangles are P-wave arrival picking results on the local window by different picking methods: (a) wavelet-transform-based approach, (b) PphasePicker algorithm, (c) STAFD/LTAFD algorithm, and (d) Deep learning method.

TABLE 2. The field picking results between non-local-window picking and local-window picking.

Method	complete waveform $M_{\|Error\|<=0.1}$	local window $N_{\|Error\|<=0.1}$	$EM = \frac{N_{\|Error\|<=\varepsilon} - M_{\|Error\|<=\varepsilon}}{N_{\|Error\|<=\varepsilon}}$
Wavelet-transform-based approach	713	864	17.5%
PphasePicker algorithm	506	811	37.6%
STAFD/LTAFD algorithm	80	213	62.4%
Deep learning method	25	47	46.8%

a local window that contains both the main components of the signal and a small scale. Therefore, the method proposed in this artilce to convert the waveform into a picture and use faster-RCNN to detect the local window can effectively solve this problem, thereby enhancing the accuracy of P-wave arrival picking. However, to implement

TABLE 3. The comparative experimental results of P-wave arrival picking of one field seismic event.

Picking algorithm	Picking on the complete waveform				Picking by targeted detecting the local window using faster-RCNN			
	Maximum error/(s)	Mean error/(s)	Minimum error/(s)	Count of the trace with an error of less than 0.1s	Maximum error/(s)	Mean error/(s)	Minimum error/(s)	Count of the trace with an error of less than 0.1s
Wavelet-transform-based approach	5.324	1.670	0	38	0.380	0.051	0	74
PphasePicker algorithm	8.826	2.304	0.002	8	0.186	0.034	0	73
STAFD/LTAFD algorithm	9.878	1.345	0.016	3	0.992	0.4577	0.012	16
Deep learning method	3.649	2.383	0.347	0	1.076	0.639	0.010	7

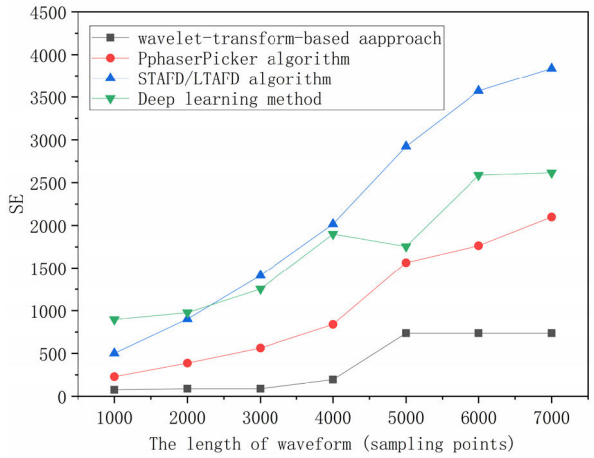

FIGURE 15. The relation between the P-wave picking precision and the length of the waveform.

this method requires a sizeable marked dataset, and the actual application effect also changes with the size of the dataset.

For future research, the time-frequency spectra could be utilized to enhance the anti-noise ability the arrival picking further. Besides, the neighbor traces can also be used to constrain the local window selection and the final picked arrivals [38].

V. CONCLUSION

P-wave arrival picking is an essential step in seismic source location and focal mechanism calculation. There are many automatic algorithms for picking the P-wave arrivals. However, these automatic algorithms are not always accurate and may even yield results that are far from the truth. The main ways to improve the precision of P-wave arrival picking include optimizing the picking algorithms and preprocessing the waveform. Therefore, this article proposes a method to enhance the accuracy of P-wave arrival picking by detecting local window from the waveform through deep learning.

This deep learning method is based on faster-RCNN, a reliable object detection algorithm. The idea of this method is to convert the seismic waveform recorded by the station into a picture and train the faster-RCNN model with the calibrated local window. The trained faster-RCNN can be used to detect the local window of those new seismic records and picking P-wave arrival in the local window. The local window is a short waveform that intercepts the main components of the original waveform.

In order to verify the effectiveness of the method proposed in this article, we selected four kinds of automatic P-wave arrival picking algorithms (wavelet-transform-based approach, PphasePicker algorithm, STAFD/LTAFD algorithm, and deep learning method) to conduct experiments in synthetic seismic records and field seismic records, respectively. The synthetic experimental results show that the method proposed in this article can improve the picking capacity of the four methods by 99.8%, 94.8%, 98.4%, and 86.7%, respectively. And the field experimental results show that the method proposed in this article can improve the picking capacity of the four methods by 17.5%, 37.6%, 62.4%, and 46.8%, respectively. Therefore, no matter which algorithm is used, the picking error in the local window is reduced clearly. At the same time, the experiment of exploring the correlation between the waveform size and the picking accuracy

also shows that the method of detecting the local window to enhance the P-wave arrival picking accuracy is feasible.

ACKNOWLEDGMENT

The authors thank the editor, assistant editor, and anonymous reviewers for their careful reviews and insightful remarks.

REFERENCES

[1] R. V. Allen, "Automatic earthquake recognition and timing from single traces," *Bull. Seismol. Soc. Amer.*, vol. 68, no. 5, pp. 1521–1532, 1978.
[2] N. Maeda, "A method for reading and checking phase time in auto-processing system of seismic wave data," *Zisin, J. Seismol. Soc. Jpn. 2nd Ser.*, vol. 38, no. 3, pp. 365–379, 1985.
[3] L. Han, J. Wong, and J. C. Bancroft, "Time picking and random noise reduction on microseismic data," *CREWES Res. Rep.*, vol. 21, pp. 1–13, Jan. 2009.
[4] S. Gaci, "The use of wavelet-based denoising techniques to enhance the first-arrival picking on seismic traces," *IEEE Trans. Geosci. Remote Sens.*, vol. 52, no. 8, pp. 4558–4563, Aug. 2014.
[5] F. Coppens, "First arrival picking on common-offset trace collections for automatic estimation of static corrections," *Geophys. Prospecting*, vol. 33, no. 8, pp. 1212–1231, Dec. 1985.
[6] J. I. Sabbione and D. Velis, "Automatic first-breaks picking: New strategies and algorithms," *Geophysics*, vol. 75, no. 4, pp. V67–V76, Jul. 2010.
[7] L. Küperkoch, T. Meier, J. Lee, and W. Friederich, "Automated determination of P-phase arrival times at regional and local distances using higher order statistics," *Geophys. J. Int.*, vol. 181, no. 2, pp. 1159–1170, 2010.
[8] X. Lou, S. van der Lee, and S. Lloyd, "AIMBAT: A Python/Matplotlib tool for measuring teleseismic arrival times," *Seismol. Res. Lett.*, vol. 84, no. 1, pp. 85–93, Jan. 2013.
[9] F. Li*, J. Rich, K. J. Marfurt, and H. Zhou, "Automatic event detection on noisy microseismograms," in *Proc. Soc. Explor. Geophysicists Int. Expo. 84th Annu. Meeting SEG*, Aug. 2014, pp. 776–780.
[10] J. Akram, D. Eaton, and A. St. Onge, "Automatic event-detection and time-picking algorithms for downhole microseismic data processing," in *Proc. 4th EAGE Passive Seismic Workshop*, Mar. 2013, p. cp-337.
[11] J. Akram, "Downhole microseismic monitoring: processing, algorithms and error analysis," M.S. thesis, Univ. Calgary, Calgary, AB, Canada, 2014, unpublished. [Online]. Available: https://prism.ucalgary.ca/handle/11023/1408, doi: 10.11575/PRISM/25742.
[12] K. S. Anant and F. U. Dowla, "Wavelet transform methods for phase identification in three-component seismograms," *Bull. Seismol. Soc. Amer.*, vol. 87, no. 6, pp. 1598–1612, 1997.
[13] J. J. Galiana-Merino, J. L. Rosa-Herranz, and S. Parolai, "Seismic *P* phase picking using a kurtosis-based criterion in the stationary wavelet domain," *IEEE Trans. Geosci. Remote Sens.*, vol. 46, no. 11, pp. 3815–3826, Nov. 2008.
[14] V. Kapetanidis and P. Papadimitriou, "Estimation of arrival-times in intense seismic sequences using a master-events methodology based on waveform similarity," *Geophys. J. Int.*, vol. 187, no. 2, pp. 889–917, Nov. 2011.
[15] X. Qu, T. Azuma, H. Imoto, R. Raufy, H. Lin, H. Nakamura, S. Tamano, S. Takagi, S.-I. Umemura, I. Sakuma, and Y. Matsumoto, "Novel automatic first-arrival picking method for ultrasound sound-speed tomography," *Jpn. J. Appl. Phys.*, vol. 54, no. 7S1, Jul. 2015, Art. no. 07HF10.
[16] Q. Liu, S. Bose, H. P. Valero, R. G. Shenoy, and A. Ounadjela, "Detecting small amplitude signal and transit times in high noise: Application to hydraulic fracture monitoring," in *Proc. Int. Geosci. Remote Sens. Symp. (IGARSS)*, vol. 4, 2009, p. IV-530.
[17] D. E. Wagner, J. W. Ehlers, and J. Veezhinathan, "First break picking using neural networks," in *Proc. SEG Tech. Program Expanded Abstr., Soc. Explor. Geophysicists*, 1990, pp. 370–373.
[18] H. Dai and C. MacBeth, "The application of back-propagation neural network to automatic picking seismic arrivals from single-component recordings," *J. Geophys. Res., Solid Earth*, vol. 102, no. B7, pp. 15105–15113, Jul. 1997.
[19] H. Dai and C. MacBeth, "Automatic picking of seismic arrivals in local earthquake data using an artificial neural network," *Geophys. J. Int.*, vol. 120, no. 3, pp. 758–774, Mar. 1995.
[20] Y. Chen, "Automatic microseismic event picking via unsupervised machine learning," *Geophys. J. Int.*, vol. 212, no. 1, pp. 88–102, Jan. 2018.
[21] T. Perol, M. Gharbi, and M. Denolle, "Convolutional neural network for earthquake detection and location," *Sci. Adv.*, vol. 4, no. 2, pp. 2–10, 2018.
[22] Z. E. Ross, M.-A. Meier, and E. Hauksson, "PWave arrival picking and first-motion polarity determination with deep learning," *J. Geophys. Res., Solid Earth*, vol. 123, no. 6, pp. 5120–5129, Jun. 2018.
[23] W. Zhu, S. M. Mousavi, and G. C. Beroza, "Seismic signal denoising and decomposition using deep neural networks," *IEEE Trans. Geosci. Remote Sens.*, vol. 57, no. 11, pp. 9476–9488, Nov. 2019.
[24] Y. Chen, G. Zhang, M. Bai, S. Zu, Z. Guan, and M. Zhang, "Automatic waveform classification and arrival picking based on convolutional neural network," *Earth Space Sci.*, vol. 6, no. 7, pp. 1244–1261, Jul. 2019.
[25] S. M. Mousavi, W. Zhu, Y. Sheng, and G. C. Beroza, "CRED: A deep residual network of convolutional and recurrent units for earthquake signal detection," *Sci. Rep.*, vol. 9, no. 1, pp. 1–14, 2019.
[26] Y. Zhou, H. Yue, Q. Kong, and S. Zhou, "Hybrid event detection and phase-picking algorithm using convolutional and recurrent neural networks," *Seismol. Res. Lett.*, vol. 90, no. 3, pp. 1079–1087, May 2019.
[27] S. Qu, Z. Guan, E. Verschuur, and Y. Chen, "Automatic high-resolution microseismic event detection via supervised machine learning," *Geophys. J. Int.*, vol. 218, no. 3, pp. 2106–2121, Sep. 2019.
[28] S. Zu, H. Zhou, W. Mao, D. Zhang, C. Li, X. Pan, and Y. Chen, "Iterative deblending of simultaneous-source data using a coherency-pass shaping operator," *Geophys. J. Int.*, vol. 211, no. 1, pp. 541–557, Oct. 2017.
[29] H. Zhang, C. Thurber, and C. Rowe, "Automatic P-Wave arrival detection and picking with multiscale wavelet analysis for single-component recordings," *Bull. Seismol. Soc. Amer.*, vol. 93, no. 5, pp. 1904–1912, Oct. 2003.
[30] *Northern California Earthquake Data Center, NCEDC*, UC Berkeley Seismol. Lab., Berkeley, CA, USA, 2014.
[31] S. Ren, K. He, R. Girshick, and J. Sun, "Faster R-CNN: Towards real-time object detection with region proposal networks," in *Proc. Adv. Neural Inf. Process. Syst.*, 2015, pp. 91–99.
[32] S. Ren, K. He, R. Girshick, and J. Sun, "Faster R-CNN: Towards real-time object detection with region proposal networks," *IEEE Trans. Pattern Anal. Mach. Intell.*, vol. 39, no. 6, pp. 1137–1149, Jun. 2017.
[33] B. Li, J. Yan, W. Wu, Z. Zhu, and X. Hu, "High performance visual tracking with Siamese region proposal network," in *Proc. IEEE Conf. Comput. Vis. Pattern Recognit.*, Jun. 2018, pp. 8971–8980.
[34] C. D. Saragiotis, L. J. Hadjileontiadis, I. T. Rekanos, and S. M. Panas, "Automatic P phase picking using maximum kurtosis and κ-statistics criteria," *IEEE Geosci. Remote Sens. Lett.*, vol. 1, no. 3, pp. 147–151, Jul. 2004.
[35] J. Zhang, Y. Tang, and H. Li, "STA/LTA fractal dimension algorithm of detecting the P-wave arrival," *Bull. Seismol. Soc. Amer.*, vol. 108, no. 1, pp. 230–237, Feb. 2018.
[36] J. Tronicke, "The influence of high frequency uncorrelated noise on first-break arrival times and crosshole traveltime tomography," *J. Environ. Eng. Geophys.*, vol. 12, no. 2, pp. 173–184, Jun. 2007.
[37] E. Kalkan, "An Automatic P-phase arrival-time picker," *Bull. Seismol. Soc. Amer.*, vol. 106, no. 3, pp. 971–986, Jun. 2016.
[38] G. Zhang, C. Lin, and Y. Chen, "Convolutional neural networks for microseismic waveform classification and arrival picking," *Geophysics*, vol. 85, no. 4, pp. WA227–WA240, Jul. 2020.

ZHENGXIANG HE received the B.S. degree in mining engineering from the School of Resources and Civil Engineering, Northeastern University, Shenyang, China, in 2016, and the M.S. degree in mineral engineering from the School of Resources and Safety Engineering, Central South University, Changsha, China, in 2019, where he is currently pursuing the Ph.D. degree. His research interests include intelligent mining, microseismic signals processing, focal mechanism, and safety mining.

PINGAN PENG received the B.S., M.S., and Ph.D. degrees in mining engineering from Central South University, Changsha, China, in 2011, 2014, and 2019, respectively. He is currently with the School of Resources and Safety Engineering, Central South University. He has published a number of research articles in refereed international journals and magazines. His current research interests include microseismic monitoring in engineering, deep learning, microseismic waveform processing, and rock mechanics. He is also a member of the Nonferrous Metals Society of China (NFSOC), the Chinese Society for Rock Mechanics and Engineering (CSRME), the American Rock Mechanics Association (ARMA), and the International Society of Rock Mechanics (ISRM). His awards and honors include the First Prize of the Technical Innovation Award from the China Nonferrous Metals Industry Association, the Mittal Outstanding Student Innovation, and the Entrepreneurship Award. He serves as a Reviewer for IEEE Access, *Ore Geology Reviews*, *Sensors*, and *Sustainability*.

LIGUAN WANG received the B.S. and M.S. degrees from Central South University, Changsha, China, in 1985 and 1988, respectively, and the Ph.D. degree from Akita University, Japan, in 2002, all in mining engineering. He is currently a Professor with the School of Resource and Safety Engineering, Central South University. He has published more than 200 articles in various refereed journals. His current research interests include digital mining, mining safety, and intelligent mining. He is also the Principal Investigator of the China National Key Research and Development Program and a Committee Member of the Nonferrous Metals Society of China (NFSOC). He has won two prizes of the National Science and Technology Progress Award and 16 prizes of the Ministerial Science and Technology Progress Award in China.

YUANJIAN JIANG received the B.S. and M.S. degrees in mining engineering from Central South University, Changsha, China, in 2016 and 2019, respectively, where he is currently pursuing the Ph.D. degree with the School of Resources and Safety Engineering. His research interests include microseismic source location, microseismic wave velocity inversion, computer algorithm, and machine learning.